

Observational constraints on cosmological solutions of $f(Q)$ theories

Ismael Ayuso^{1,*}, Ruth Lazkoz^{2,†} and Vincenzo Salzano^{3,‡}

¹*Departamento de Física and Instituto de Astrofísica e Ciências do Espaço, Faculdade de Ciências, Universidade de Lisboa, Edifício C8, Campo Grande, 1769-016 Lisboa, Portugal*

²*Department of Theoretical Physics, University of the Basque Country UPV/EHU, P.O. Box 644, 48080 Bilbao, Spain*

³*Institute of Physics, Faculty of Mathematics and Physics, University of Szczecin, Wielkopolska 15, 70-451 Szczecin, Poland*



(Received 17 December 2020; accepted 3 February 2021; published 8 March 2021)

Over the last years some interest has been gathered by $f(Q)$ theories, which are new candidates to replace Einstein's prescription for gravity. The nonmetricity tensor Q allows to put forward the assumption of a free torsionless connection and, consequently, new degrees of freedom in the action are taken into account. This work focuses on a class of $f(Q)$ theories, characterized by the presence of a general power-law term which adds up to the standard (linear in) Q term in the action, and on new cosmological scenarios arising from them. Using the Markov chain Monte Carlo method, we carry out statistical tests relying upon background data such as Type Ia supernovae luminosities and direct Hubble data (from cosmic clocks), along with cosmic microwave background shift and baryon acoustic oscillations data. This allows us to perform a multifaceted comparison between these new cosmologies and the (concordance) Λ CDM setup. We conclude that, at the current precision level, the best fits of our $f(Q)$ models correspond to values of their specific parameters which make them hardly distinguishable from our general relativity “échantillon,” that is, Λ CDM.

DOI: [10.1103/PhysRevD.103.063505](https://doi.org/10.1103/PhysRevD.103.063505)

I. INTRODUCTION

The Universe is dominated by the weakest force of all, that is, the gravitational interaction, and it is through a deep comprehension of the latter that we will improve our understanding of the former. Currently, the most successful theory concerning the behavior and evolution of the Universe is general relativity (GR) [1,2], which passes all tests up to the solar system scale with flying colors [3,4]. However, when we try to explain the physics of the cosmos on larger scales, it becomes mandatory to consider more exotic kinds of energy and matter than the standard sources of geometry. In this way, and under the uncontroversial assumption of homogeneity and isotropy in a GR ruled Universe, the Λ CDM model provides a quite worthy chronicle of our Universe driven by new unusual components (as we have anticipated): dark matter and dark energy. The first one accounts proficiently for structure formation and evolution, whereas the second one performs quite well at explaining the current accelerated expansion of the Universe.

Nevertheless, we cannot describe the physics of our Universe by just scraping its surface: when we examine the

Λ CDM model in the light of the whole assortment of evidences available, we realize that, unfortunately, its two main components lead to new problems [5–11]. In particular, volumes have been written about the shortcomings of the specific type of dark energy on which the model relies, the cosmological constant (Λ). Needless to say, it is not our purpose to dwell into this matter, but rather adopt a different perspective.

Modified theories of gravity have precisely been proposed along the years to tackle those and other challenges [12–16]. Among the different starting points considered in the vast literature, we will embrace that of metric-affine geometry, which generalizes the Riemannian geometry approach adopted in GR [17]. The connection then becomes a nonstandard free variable at the same level as the metric, and hence it is not necessarily of the Levi-Civita type. Broadly speaking, this freedom in the features of the connection brings a rich phenomenology related to the transformations which objects of physico-mathematical nature that undergo along a displacement [18,19].

Specifically, we are going to study theories of modified gravity based on nonmetricity [20], a quantity which measures how the length of a vector changes when it is transported. After offering new views on some theoretical aspects of this ample framework, we will resort to observational tests so as to draw conclusions on the (statistical and physical) reliability of some specific models.

*iayuso@fc.ul.pt

†ruth.lazkoz@ehu.es

‡vincenzo.salzano@usz.edu.pl

The connection between theory and observations arises from the possibility to write useful prescriptions for cosmological applications. Specifically, just following pertinent generalizations of otherwise standard procedures, one can compute the Hubble parameter analytically [21] for a class of nonmetricity spacetime geometries. The statistical analysis is performed using state-of-the-art cosmological probes under the assumption of some specific matter-energy content so that the candidate models offer (*a priori*) viable modified gravity candidates to describe the cosmological background. The procedure progresses from the initial expression of the Hubble parameter to the construction of various cosmological distances (luminosity distance, angular diameter distance, etc.). Interestingly, the GR limit of these modified gravity frameworks will be easily recognizable, thus allowing for a neat statistical analysis.

Let us now offer a guide to the organization of this paper. In Sec. II, we will produce a convenient introduction to nonmetricity theories of modified gravity. In this very section, and for the sake of motivation of further steps, we will revisit how one can construct genuine settings based solely on nonmetricity which, however, do mimic GR perfectly at all levels.

We will move then to Sec. III and build upon the previous discussion to offer more general scenarios, still based on nonmetricity, but not necessarily fully equivalent to GR. Upon very general hypotheses, we will be able to present the new versions of the Friedman and Raychaudhuri equations. An intermediate step within this section deals with possible equivalences between these new frameworks and GR at the cosmological level. This gives us a flavor of how peculiar the consequences of nonmetricity are. The findings of this exercise will serve as an inspiration to propose (obtain) the Hubble parameter of the final specific model we shall work with. Our models will display a characteristic set of parameters: all but one are very standard, and it is upon switching off the unusual one that we recover the customary GR sort of cosmological evolution.

A statistical analysis based on the Markov chain Monte Carlo (MCMC) procedure (see Sec. IV) will yield tight enough constraints on the parameters, and results will be shown in Sec. VI. The best fits, errors, and statistical criteria will be driven by supernovae type Ia luminosity data and modulated by direct Hubble (cosmic clocks), cosmic microwave background (CMB) shift, and baryon acoustic oscillation (BAO) data (head to Sec. V for further details). Last, we will dissertate about our conclusions in Sec. VII.

II. SYMMETRIC TELEPARALLEL GRAVITY

Currently, the gravitational interaction is interpreted as a geometrization of a manifold allowed by the equivalence principle. Put in other words, gravity is a physical manifestation of the mathematical conformation of that

manifold. For the case of GR, a spacetime comes about upon endowing a manifold with a prescription to measure distances that mathematically takes the form of the metric tensor $g_{\mu\nu}$ and is the only object where gravitational effects are encoded.

Interestingly, though, the metric does not happen to be the only fundamental object allowing to characterize the geometry of a manifold. Furthermore, there is an affine structure associated with how objects move about the manifold; this is represented by a connection, $\Gamma_{\mu\nu}^{\alpha}$, a degree of freedom (d.o.f) which may be subject to certain specifications imposed by the theoretical setting. For instance, in GR, the connection amounts to a combination of (conventional) derivatives of the metric tensor (Christoffel symbols), but other options are possible if one ventures beyond the classical realm in gravity [22].

Hence, provided that the connection is not (so to speak) geometrically trivial, one can define two further fundamental objects conveying additional relevant information about it [23]. The first one is the nonmetricity tensor,

$$Q_{\alpha\mu\nu} \equiv \nabla_{\alpha} g_{\mu\nu}. \quad (1)$$

The second one is the torsion, which stems from the antisymmetric part of the connection,

$$T_{\mu\nu}^{\alpha} \equiv \Gamma_{\mu\nu}^{\alpha} - \Gamma_{\nu\mu}^{\alpha}. \quad (2)$$

If the connection is symmetric and metricity holds (i.e., when the torsion and nonmetricity tensors vanish), we recover the Levi-Civita connection; thus, gravity “à la Einstein” is restored (i.e., the metric goes back to being the only d.o.f). Conversely, in the so-called Palatini formalism (which will be addressed again below), the metric and the connection could be considered as independent objects whose relations would be given by the field equations [24,25].

In addition, and in view of the previous discussions, we can decompose a general connection $\Gamma_{\mu\nu}^{\alpha}$ as follows [18,23]:

$$\Gamma_{\mu\nu}^{\alpha} = \left\{ \begin{matrix} \alpha \\ \mu\nu \end{matrix} \right\} + K^{\alpha}_{\mu\nu} + L^{\alpha}_{\mu\nu}, \quad (3)$$

where

$$K^{\alpha}_{\mu\nu} = \frac{1}{2} T^{\alpha}_{\mu\nu} + T_{(\mu}^{\alpha}{}_{\nu)} \quad (4)$$

is the contortion, and

$$L^{\alpha}_{\mu\nu} = \frac{1}{2} Q^{\alpha}_{\mu\nu} - Q_{(\mu}^{\alpha}{}_{\nu)} \quad (5)$$

is the disformation. The latter will be the relevant magnitude for this work, as it measures how much the symmetric

part of the (general) connection deviates from the Levi-Civita connection, $\{\overset{\alpha}{\mu\nu}\}$. In any case, and as usual, the curvature will be determined by the Riemann tensor in this way,

$$R^\alpha{}_{\beta\mu\nu}(\Gamma) = \partial_\mu \Gamma^\alpha{}_{\nu\beta} - \partial_\nu \Gamma^\alpha{}_{\mu\beta} + \Gamma^\alpha{}_{\mu\lambda} \Gamma^\lambda{}_{\nu\beta} - \Gamma^\alpha{}_{\nu\lambda} \Gamma^\lambda{}_{\mu\beta}. \quad (6)$$

However, all this information will be of little use without a theory of gravity, so let us make some progress by introducing GR through the Hilbert-Einstein action,

$$S_{\text{GR}} = \frac{1}{16\pi G} \int d^x \sqrt{-g} R(\{\}), \quad (7)$$

where $R(\{\})$ is the scalar of curvature upon the specific choice of the Levi-Civita connection in Eq. (6). This action has a special property. Let us think for a moment that we readdress it but using rather now the general scalar of curvature $R(\Gamma)$, instead of $R(\{\})$, and then study this “alternative action” in the Palatini formalism. Upon the exercise of varying the action with respect to the metric on the one hand, and the connection on the other hand, we obtain two sets of equations which are not blind to each other: they specifically fix the connection to be the Levi-Civita one. Summarizing, if GR is our gravitational theory, both formalisms yield the same equations of motion because nonmetricity and torsion vanish. Nevertheless, this is but an exception of GR which will not be true for theories of modified gravity in general, and yet it can be used to our advantage. Indeed, incorporating the connection as a new d.o.f on the framework of modified gravity opens a complete new range of theoretical settings to explore.

The next step in our journey is to study how the Riemann tensor is transformed by a shift of the connection of the form $\hat{\Gamma}^\alpha{}_{\beta\mu\nu} = \Gamma^\alpha{}_{\mu\nu} + \Omega^\alpha{}_{\mu\nu}$ where $\Omega^\alpha{}_{\mu\nu}$ is an arbitrary tensor which encodes the transformation. Specifically,

$$\begin{aligned} \hat{R}^\alpha{}_{\beta\mu\nu}(\hat{\Gamma}) &= R^\alpha{}_{\beta\mu\nu}(\Gamma) + T^\lambda{}_{\mu\nu} \Omega^\alpha{}_{\lambda\beta} \\ &\quad + 2\nabla_{[\mu} \Omega^\alpha{}_{\nu]\beta} + 2\Omega^\alpha{}_{[\mu|\lambda]} \Omega^\lambda{}_{\nu]\beta}, \end{aligned} \quad (8)$$

where ∇ is the covariant derivative associated to Γ .

Upon inspection of the latter, one can follow on the steps of [18] to end up realizing the existence of a theory which is fully equivalent to GR (as obtained from the Levi-Civita connection) but coming instead and solely from the disformation (the part of the connection related to the nonmetricity).¹ This requirement translates into $\Gamma = \{\}$, $T^\lambda{}_{\mu\nu} = 0$, and $\Omega^\alpha{}_{\mu\nu} = L^\alpha{}_{\mu\nu}$. If we replace those expressions into Eq. (8), it becomes

¹Note that in this theory the torsion plays no role whatsoever.

$$R^\alpha{}_{\beta\mu\nu}(\hat{\Gamma}) = R^\alpha{}_{\beta\mu\nu}(\{\}) + 2\nabla_{[\mu}^{\{\}} L^\alpha{}_{\nu]\beta} + 2L^\alpha{}_{[\mu|\lambda]} L^\lambda{}_{\nu]\beta}, \quad (9)$$

where the superindex in $\nabla^{\{\}}$ specifies the covariant derivative defined from the Levi-Civita connection. The latter and other intermediate steps conform our alternative and hopefully pedagogical explanation about how to build such theory.

Again, inspection suggests additional requirements are needed in order to eventually reach the goal, so in this spirit let us demand our spacetime to be flat by the constraint $R^\alpha{}_{\beta\mu\nu}(\hat{\Gamma}) = 0$, which reduces the connection to the Weitzenböck form [26,27]. The theories formulated in these frameworks are referred to as teleparallel due to a well-defined notion of parallelism² as a consequence of the vanishing of total curvature [18,32,33].

As the literature proves, in this symmetric teleparallel framework [34], it is possible to find a theory which reproduces exactly GR but through the nonmetricity tensor, $Q_{\alpha\mu}$ which mediates the gravitational force, instead of resorting to curvature for that task [18]. This special case is called symmetric teleparallel equivalent general relativity (STEGR).

But we wish to throw further light into this fact, and to that end we perform a contraction of Eq. (9) which can be used to rewrite $R(\{\})$ (the piece we eventually need to show the equivalence at the Lagrangian level),

$$\begin{aligned} 0 &= R(\{\}) + \nabla_\alpha^{\{\}} (Q^\alpha - \tilde{Q}^\alpha) + \frac{1}{4} Q^{\alpha\beta\gamma} Q_{\alpha\beta\gamma} \\ &\quad - \frac{1}{2} Q^{\gamma\alpha\beta} Q_{\alpha\gamma\beta} - \frac{1}{4} Q^\alpha Q_\alpha + \frac{1}{2} \tilde{Q}^\alpha Q_\alpha, \end{aligned} \quad (10)$$

where $Q_\alpha = Q_\alpha{}^\mu{}_\mu$ and $\tilde{Q}_\alpha = Q^\mu{}_\alpha{}^\mu$. It is convenient now to simplify the latter expression by defining the nonmetricity scalar Q as³

$$Q = \frac{1}{4} Q^{\alpha\beta\gamma} Q_{\alpha\beta\gamma} - \frac{1}{2} Q^{\gamma\alpha\beta} Q_{\alpha\gamma\beta} - \frac{1}{4} Q^\alpha Q_\alpha + \frac{1}{2} \tilde{Q}^\alpha Q_\alpha. \quad (11)$$

Therefore, for symmetric (torsionless) and flat constraints, we get

$$R(\{\}) = -Q - \nabla_\alpha^{\{\}} (Q^\alpha - \tilde{Q}^\alpha), \quad (12)$$

²As a bonus, that this formulation can be regarded as a “translational gauge theory” [28–31].

³However, the most general even-parity second order quadratic form of the nonmetricity is

$$\begin{aligned} \mathcal{Q} &= \frac{c_1}{4} Q_{\alpha\mu\nu} Q^{\alpha\mu\nu} - \frac{c_2}{2} Q_{\alpha\mu\nu} Q^{\mu\alpha\nu} - \frac{c_3}{4} Q_\alpha Q^\alpha \\ &\quad + \frac{c_4}{2} Q_\alpha \tilde{Q}^\alpha + (c_5 - 1) \tilde{Q}_\alpha \tilde{Q}^\alpha, \end{aligned}$$

which is a generalization of Eq. (11) that gets recovered by setting $c_1 = c_2 = c_3 = c_4 = 1$.

where $\nabla_a^{\{\}}$ is a total divergence term. Continuing with this lengthy scheme, we can verify that if we take the scalar of curvature obtained from the Levi-Civita connection appearing in Eq. (7) and we replace it with Eq. (12), we in fact build a theory which is equivalent to GR up to a total derivative in the action, which, in any case, does not contribute to the equations of motion,

$$\begin{aligned} S_{\text{GR}} &= \frac{1}{16\pi G} \int d^4x \sqrt{-g} R(\{\}) \\ &= -\frac{1}{16\pi G} \int d^4x \sqrt{-g} Q = S_{\text{STEGR}}. \end{aligned} \quad (13)$$

Therefore, the STEGR theory and GR are equivalent frameworks of gravity but formulated with R and Q , respectively. Obviously, cosmological models following from these two settings are completely identical, and cosmological observations would no offer hints as to which is the underlying theory. However, we now are in a position which allows us to go one step beyond and build $f(Q)$ models, close enough to GR to make sense, but at the same time, different enough so that small modifications could ideally be spotted. In this sense, we want to stress that theories stemming from actions based on Q have only began to be explored in what regards observations. For instance, a previous work by some of us [35] adopted a more phenomenological perspective by putting forward expressions for $f(Q)$ directly as functions of the redshift with some parameters which cannot be readily associated to a specific matter/energy content. Of course, both routes are complementary and for this reason, we feel that continuing to explore statistical examinations of the free parameters of $f(Q)$ cosmologies in the light of astrophysical data could help us discuss the suitability of $f(Q)$ in general.

III. $F(Q)$ COSMOLOGIES

Following the justification offered in the previous sections, we generalize now the STEGR action as follows:

$$S = \int d^4x \sqrt{-g} \left[-\frac{1}{2} f(Q) + \mathcal{L}_M \right], \quad (14)$$

where STEGR is directly recovered for $f(Q) = Q/8\pi G$.

Analogously to [21], we are going to work in the coincident gauge, which allows to use a null connection, that is,

$${}_{cg}\Gamma_{\mu\nu}^\alpha = 0 \rightarrow \nabla_\alpha g_{\mu\nu} = \partial_\alpha g_{\mu\nu}. \quad (15)$$

Besides, we will consider a spatially flat Friedmann-Lemaître-Robertson-Walker spacetime, as the most used homogeneous an isotropic standard spacetime to describe the Universe on large scales,

$$ds^2 = -N^2(t)dt^2 + a^2(t)[dx^2 + dy^2 + dz^2], \quad (16)$$

for which the nonmetricity scalar reads

$$Q = 6 \frac{H^2}{N^2}. \quad (17)$$

As shown in [36], $f(Q)$ theories let us fix a particular lapse function because Q retains a residual time-reparametrization invariance, in spite of which we have already used diffeomorphisms to select the coincident gauge. Therefore, and for simplicity, we will take this to our advantage and choose $N(t) = 1$. Then, the cosmological equations become

$$6f_Q H^2 - \frac{1}{2} f = \rho, \quad (18)$$

$$(12H^2 f_{QQ} + f_Q) \dot{H} = -\frac{1}{2}(\rho + p), \quad (19)$$

where the subindex denotes derivatives with respect to Q . Examination shows that we can reproduce exactly the GR background behavior under the prescription

$$Q f_Q - \frac{1}{2} f = \frac{3H^2}{8\pi G} = \frac{Q}{16\pi G}, \quad (20)$$

which implies

$$f(Q) = \frac{1}{8\pi G} (Q + M\sqrt{Q}), \quad (21)$$

where M is a constant which can be interpreted as a mass scale [21]. The analogy between the particular case with $M = 0$ and GR should be not surprising at all, because it corresponds to the STEGR framework we already discussed in the previous section. But the $M \neq 0$ case represents a whole class of theories with the same background as GR whose differences do not show up at the background level, although they do it at the perturbation level.

An alternative route is to put forward an ansatz for $f(Q)$ that includes Eq. (21) as a particular case in the hope that this analytical extension will let us integrate Eqs. (18) and (19) and so progress will be made possible. This happens to be the case for the proposal presented in [21]

$$f(Q) = \frac{1}{8\pi G} \left[Q - 6\lambda M^2 \left(\frac{Q}{6M^2} \right)^\alpha \right], \quad (22)$$

where λ and α are dimensionless parameters and $M \neq 0$. Interestingly, different values of α can be chosen to construct solutions depicting new early or late Universe behaviors.

From Eq. (22) and using Eq. (17), the Friedmann equation (18) can be integrated to yield

$$H^2 \left[1 + (1 - 2\alpha)\lambda \left(\frac{H^2}{M^2} \right)^{\alpha-1} \right] = \frac{8\pi G}{3} \rho. \quad (23)$$

Note that a background evolution identical to that of GR is recovered for either $\lambda = 0$ or $\alpha = 1/2$. In addition, the case for $\alpha = 1$ follows the same dynamics than GR after a redefinition of G .

In this paper, though, we will follow [21] and set the focus on the $\alpha = -1$ case, which leads to a solution with two possible branches,

$$H_{\pm}^2 = \frac{4\pi G}{3} \rho \left(1 \pm \sqrt{1 - \frac{27\lambda M^4}{(4\pi G\rho)^2}} \right), \quad (24)$$

where ρ is the sum of all energy densities (as customary it will be regarded as positive). The correction with respect to the GR case becomes larger as ρ decreases, so the new degree of freedom plays the effective role of dark energy. Note the considerable level of nonlinearity at play in Eq. (24).

From now on, and in order to be able to exploit the predicting capabilities of an assortment of cosmological data sets, we are going to consider our Universe's evolution is driven by the three usual kinds of matter energy: cosmic dust, radiation, and a cosmological constant.

The explicit presence of a cosmological constant might seem redundant or unnecessary, as we rather want to explore geometric corrections that mimic its effect. However, it will become clear that, as far as statistical comparisons are concerned, the presence of such a term renders the whole analysis far more palpable.

Additionally, the whole lot of standard matter-energy fields will satisfy the continuity equation, that is,

$$\dot{\rho} = -3H(\rho + p), \quad (25)$$

where the dot denotes derivation with respect to cosmic time. With our choices, ρ reads

$$\rho = \frac{3H_0^2}{8\pi G} [\Omega_{\Lambda} + \Omega_m(1+z)^3 + \Omega_r(1+z)^4], \quad (26)$$

where we let Ω_{Λ} , Ω_m , and Ω_r stand for current values of the fractional densities of the three cosmological fluids comprising our matter-energy lot. Under this whole set of prescriptions, the way to recover the Λ CDM setting, for the positive branch, is

$$H_+^2|_{\Omega_Q=0} = H_{\Lambda\text{CDM}}^2. \quad (27)$$

We will also resort to the customary ‘‘normalization’’ of the Hubble parameter so as to lighten the notation whenever possible,

$$E(z=0) = \frac{H_{\pm}(z=0)}{H_0} = 1. \quad (28)$$

This gives us

$$-\frac{M^4\lambda}{H_0^4} = \frac{1}{3}(1 - \Omega_{\Lambda} - \Omega_m - \Omega_r) \equiv \frac{\Omega_Q}{3}, \quad (29)$$

which can be seen to hold for both branches (obviously, the standard Λ CDM normalization condition follows from choosing Ω_Q). Besides, and consequently, we will say that Ω_{Λ} , Ω_m , and Ω_r are primary parameters, in contrast to Ω_Q which is a derived one.

In addition, let us remark a peculiarity from the previous normalization. When it is carried out for the positive branch, one of the intermediate steps is

$$\sqrt{1 - \frac{12\lambda M^4}{H_0^4(\Omega_{\Lambda} + \Omega_m + \Omega_r)^2}} = \frac{2 - \Omega_{\Lambda} - \Omega_m - \Omega_r}{\Omega_{\Lambda} + \Omega_m + \Omega_r}. \quad (30)$$

Because the left side of this equation is positive, the right side must be as well. Therefore, it is also necessary to impose the condition $0 < \Omega_{\Lambda} + \Omega_m + \Omega_r < 2$, and this condition lets Ω_Q take negative values. By contrast, a healthy behavior enabling the normalization in the negative branch would demand either $\Omega_{\Lambda} + \Omega_m + \Omega_r > 2$ or $\Omega_{\Lambda} + \Omega_m + \Omega_r < 0$ (clearly, the second condition makes no sense physically).

After these convenient remarks, we can use Eq. (29) to rewrite the Hubble parameter as a function of the free parameters to be fitted at a later stage in this work,

$$H_{\pm}^2 = \frac{H_0^2}{2} [\Omega_{\Lambda} + \Omega_m(1+z)^3 + \Omega_r(1+z)^4] \times \left(1 \pm \sqrt{1 + \frac{4\Omega_Q}{[\Omega_{\Lambda} + \Omega_m(1+z)^3 + \Omega_r(1+z)^4]^2}} \right). \quad (31)$$

Note that the $\Omega_Q < 0$ case of the latter bears resemblance to the Dvali-Gabadadze-Porrati scenario with and anti-de Sitter bulk studied in [37], and therefore exploring whether our case experiences a sudden future singularity in the future may be an interesting future prospect, we will come back to this shortly.

Up to this point, we have presented a discussion as general as possible, but in the remainder, we will consider the positive branch only, because the negative one depicts a Hubble parameter which decreases as z increases and therefore seems quite unlikely to match observational evidences.

Obviously, at high redshifts, the contribution of Ω_Q becomes negligible and one recovers the usual Λ CDM Hubble parameter, as we have already mentioned. However, at the asymptotic future, one rather has

$$\lim_{\rho_m, \rho_r \rightarrow 0} H_+^2 = \frac{1}{2} H_0^2 \left[\Omega_\Lambda + \sqrt{\Omega_\Lambda^2 + 4\Omega_Q} \right] \quad (32)$$

and for the extremal case without a cosmological constant, that is, $\Omega_\Lambda = 0$, $H_{ds}^2 = H_0^2 \sqrt{\Omega_Q}$.

It is clear that in order to guarantee the physicality of our expression in this particular regime we should impose more restrictive conditions (priors), as the positivity of Ω_Q for the case without cosmological constant, or $\Omega_\Lambda^2 > -4\Omega_Q$ for the general case. This subject is related to the possible appearance of sudden cosmological singularities which we have mentioned before. Interestingly, if such singularities occurred, then the above physicality conditions would be no longer necessary, as the singularity would happen earlier than the above considered asymptotic future. Again, the parameter space could be restricted through priors to preclude such singular behavior. However, we will rather let data speak for themselves and see whether observations end up favoring parameter values capable of causing trouble in the negative redshift region (of which they really offer no control).

From a wider perspective, one could also wonder about the particular case of our $f(Q)$ model that follows from setting $\Omega_\Lambda = 0$, thus letting the effects of nonmetricity account entirely for the dark energy sector allowing us to waive the presence of a cosmological constant or any other form of dark energy altogether. Although this scenario might seem too optimistic, we will examine it too.

IV. MCMC ANALYSIS

One of the main objectives of this paper is to obtain as tight as possible constraints on the parameters of the $f(Q)$ model under study. Results will throw some light as to whether nonmetricity effects are compatible with observations, thus opening a new window of interest on the possibility of an underlying modified gravity description of our Universe. In order to narrow down our conclusions, we will combine different background astrophysical probes of known statistical relevance.

As it has been already stressed, we are sticking to the positive branch Eq. (31) of these new cosmological scenarios. The tests will be implemented using an MCMC code [38,39], which, upon minimization of a total χ^2 , will produce proficient fits of the values of Ω_m , h , Ω_Λ , Ω_Q , and Ω_b ; and, by the same token, this analysis will also produce selection criteria permitting us to draw unimpaired conclusions.

A. Priors

Our results will be obtained under the assumption of some priors, which give some room to modified gravity features, enforce the choice of the right branch, and preclude nonphysical behavior and pronounced departures from the well-established standard evolution (the Λ CDM

golden pattern). Specifically, we assume a uniform uninformative probability for values of the parameters within the intervals defined by the following:

- (i) $0 < \Omega_r < \Omega_b < \Omega_m$
- (ii) $0 < h < 1$
- (iii) $0 < \Omega_m + \Omega_\Lambda + \Omega_r < 2$

We stress again that according to our earlier discussion, and in view of these priors, Ω_Q can be either positive or negative.

But the best fits and errors alone are not all the information we can infer from the MCMC procedure. Indeed, we can also learn about the reliability of the model by invoking the evidence \mathcal{E} , also dubbed marginal likelihood or integrated likelihood. It is defined as follows:

$$\mathcal{E} = P(D|\mathcal{M}) = \int P(D|\theta, \mathcal{M})P(\theta|\mathcal{M})d\theta, \quad (33)$$

that is, it estimates the support of the (measured) data D for a given model \mathcal{M} once all possible values for the parameters θ have been considered. The evidence is generally recognized as the most reliable statistical tool for model comparison in cosmology [40], provided that wide-enough priors are chosen.

Specifically, the performance of different models is compared through the Bayes factor, that is, the ratio of their evidences,

$$\mathcal{B}_j^i = \frac{\mathcal{E}_i}{\mathcal{E}_j}. \quad (34)$$

In gross terms if $\mathcal{B}_j^i > 1$, that is, $\mathcal{E}_i > \mathcal{E}_j$ for the measured data D , then model \mathcal{M}_i is preferred over model \mathcal{M}_j .

However, it is difficult to quantify how much better (or worse) is one scenario as compared to the other. Jeffreys' scale [41] is typically adduced in this regard. According to that criterion, if $\ln \mathcal{B}_j^i < 1$, the evidence in favor of the model \mathcal{M}_i is not significant; if $1 < \ln \mathcal{B}_j^i < 2.5$, the evidence is substantial; if $2.5 < \ln \mathcal{B}_j^i < 5$, it is strong; and if $\ln \mathcal{B}_j^i > 5$, it is decisive. Nevertheless, Jeffreys' scale is not completely flawless, as discussed in [40]. Along this work, we will fix \mathcal{E}_j to be the evidence of Λ CDM to be used as a standard value, in opposite to \mathcal{E}_i , which will be the evidence of the studied model.

B. Cosmographic parameters

On the other hand, it is customary to examine other quantities which offer a clearer picture of the evolutionary features of the particular Friedmann-Lemaître-Robertson-Walker spacetime under study. In fact, once constraints on Ω_m , h , Ω_Λ , Ω_Q , and Ω_b are obtained through our MCMC procedure, we can also draw inferences on the well-known cosmographic parameters, which follow from the Taylor expansion of the scale factor,

$$a(t) = a_0 \left[1 + H_0 \Delta t - \frac{q_0}{2} H_0^2 \Delta t^2 + \frac{j_0}{3!} h_0^3 \Delta t^3 + \frac{s_0}{4!} h_0^4 \Delta t^4 + O(\Delta t^5) \right]. \quad (35)$$

In the latter, we have defined $\Delta t = t - t_0$ while q_0 , j_0 , and s_0 are the so-called deceleration, jerk, and snap parameters, respectively, evaluated at t_0 (present time) [42,43]. Explicit expressions to evaluate them can be found in many references and we just reproduce them here for the benefit of the readers,

$$q(t) = -\frac{a\ddot{a}}{\dot{a}^2} \rightarrow q(z) = -1 + (1+z) \frac{E'(z)}{E(z)}, \quad (36)$$

$$j(t) = \frac{a^2 \dot{\ddot{a}}}{\dot{a}^3} \rightarrow j(z) = (1+z)^2 \frac{E''(z)}{E(z)} + q^2(z), \quad (37)$$

$$s(t) = \frac{a^3 \ddot{\ddot{a}}}{\dot{a}^4} \rightarrow s(z) = -(1+z)j'(z) - 2j(z) - 3q(z)j(z), \quad (38)$$

where the dot and the prime denote differentiation with respect to cosmic time and z , respectively.

V. OBSERVATIONAL DATA AND STATISTICAL ANALYSIS

In this section, we put forward the cosmological data used in this work for an observational scrutiny of both Λ CDM and the $f(Q)$ given by Eq. (31). Specifically, we use Type Ia supernovae with Pantheon data, the expansion rate data from early type galaxies as cosmic chronometers with *Hubble* data, cosmic microwave background shift parameters from *Planck* 2018, and baryon acoustic oscillations data to this purpose.

We are going to proceed as follows. First, we will provide details on how to apply each probe on its own, that is, we will explain how we will construct each separate χ^2 contributing to the total one (the sum of all previous ones). Then we will find the values of the parameters which minimize each of those individual contributions (with the pertinent errors) in order to appreciate the contribution of each data set, and after this we will repeat the procedure but using the total χ^2 .

Our best fits report will be arranged in a table so as to make the conclusions readier to be drawn. We will also provide the complementary visual support of confidence contours, which inform us pictorially on the degree of correlations among parameters, the tightness of the constraints each data set suggests, and various other interpretation tools.

A. Pantheon supernovae data

This sample is one of the latest Type Ia supernovae (SNeIa) compilations [44] and it contains 1048 SNeIa at redshift $0.01 < z < 2.26$. The constraining power of SNeIa becomes manifest when used as standard candles. This can be implemented through the use of the distance modulus,

$$\mathcal{F}(z, \mathbf{x})_{\text{theo}} = 5 \log_{10} [D_L(z, \mathbf{x})] + \mu_0, \quad (39)$$

where D_L is the luminosity distance given by

$$D_L(\mathbf{x}) = (1+z) \int_0^z \frac{cdz'}{H_0 E(z', \mathbf{x})}, \quad (40)$$

and \mathbf{x} is the vector with the free parameters to be fit. Note that the factor c/H_0 can be reabsorbed into μ_0 . Then, one can construct $\Delta\mathcal{F}(\mathbf{x}) = \mathcal{F}_{\text{theo}} - \mathcal{F}_{\text{obs}}$, using for this purpose the distance modulus \mathcal{F}_{obs} associated with the observed magnitude. At this point, it may be thought that a possible χ_{SN}^2 is

$$\chi_{SN}^2(\mathbf{x}) = (\Delta\mathcal{F}(\mathbf{x}))^T \cdot C_{SN}^{-1} \cdot \Delta\mathcal{F}(\mathbf{x}). \quad (41)$$

However, the latter would contain the nuisance parameter μ_0 , which in turn is a function of the Hubble constant, the speed of light c , and the SNeIa absolute magnitude. In order to circumvent this problem, χ_{SN}^2 is marginalized analytically with respect to μ_0 as in [45], thus obtaining a new χ_{SN} estimator of the form

$$\chi_{SN}^2(\mathbf{x}) = (\Delta\mathcal{F}(\mathbf{x}))^T \cdot C_{SN}^{-1} \cdot \Delta\mathcal{F}(\mathbf{x}) + \ln \frac{S}{2\pi} - \frac{k^2(\mathbf{x})}{S}, \quad (42)$$

where C_{SN} is the total covariance matrix, S is the sum of all entries of C_{SN}^{-1} , which gives an estimation of the precision of these data independently of \mathbf{x} , and k is $\Delta\mathcal{F}(\Omega_m, \Omega_r, \Omega_\Lambda)$ but weighed by a covariance matrix with as follows:

$$k(\mathbf{x}) = (\Delta\mathcal{F}(\mathbf{x}))^T \cdot C_{SN}^{-1}. \quad (43)$$

B. Hubble data

Early time passively evolving galaxies have some peculiar features in their spectra which have been shown to correlate with their evolving stage. Thus, direct astrophysical measurements can estimate their differential ages at different redshifts and this can be finally related to the Hubble parameter. For more details, see [46–48]. Therefore, and essentially, this is a sample of 31 values of $H(z)$ for $0.07 < z < 1.965$ [49,50] to assist us in fitting the free parameters of our theoretical setting through the construction of a χ_H^2 as follows:

$$\chi_H^2 = \sum_{i=1}^{31} \frac{[H(z_i, \mathbf{x}) - H_{\text{obs}}(z_i)]^2}{\sigma_H^2(z_i)}, \quad (44)$$

where $H_{\text{obs}}(z_i)$ is the observed value at z_i , $\sigma_H(z_i)$ are the observational errors, and $H(z_i, \mathbf{x})$ is the value of a theoretical H for the same z_i with the specific parameter vector \mathbf{x} . Needless to say, for our case of interest $H(z_i, \mathbf{x})$ will be given by the positive branch of Eq. (31).

C. Cosmic microwave background data

It is common practice to condense CMB data into the so-called shift parameters [51] when examining the evolution of the cosmological background. This set of three quantities basically informs us of the position of the first peak in the temperature angular power spectrum through the ratio between its position in the model one wants to analyze and that of an Λ CDM model (standard cold dark matter). The set of shift parameters is formed by the exact expression of that quadrature ratio (an approximate yet quite accurate expression) and the normalized density fraction of baryons. We construct the χ_{CMB}^2 estimator as

$$\chi_{\text{CMB}}^2 = (\Delta\mathcal{F}^{\text{CMB}})^T \cdot C_{\text{CMB}}^{-1} \cdot \Delta\mathcal{F}^{\text{CMB}}, \quad (45)$$

where $\Delta\mathcal{F}^{\text{CMB}}$ is a vector formed by those three quantities mentioned above [51].

We have used the Planck 2018 data release [52] to obtain the shift parameters which, according to our earlier sketch, are defined as

$$R(\mathbf{x}) \equiv \sqrt{\Omega_m H_0^2} \frac{r(z_*, \mathbf{x})}{c}, \quad (46)$$

$$l_a(\mathbf{x}) \equiv \pi \frac{r(z_*, \mathbf{x})}{r_s(z_*, \mathbf{x})}, \quad (47)$$

$$\omega_b \equiv \Omega_b h^2, \quad (48)$$

where $r(z, \mathbf{x})$ is the comoving distance to z , which reads

$$r(z, \mathbf{x}) = \int_0^z \frac{c}{H(z', \mathbf{x})} dz', \quad (49)$$

and $r_s(z, \mathbf{x})$ is the comoving sound horizon, defined as

$$r_s(z, \mathbf{x}) = \int_z^\infty \frac{c_s(z')}{H(z', \mathbf{x})} dz'. \quad (50)$$

In the latter, we must take into account that the sound speed $c_s(z)$ is given by the expression

$$c_s(z) = \frac{c}{\sqrt{3(1 + \hat{R}_b(1+z)^{-1})}}, \quad (51)$$

where

$$\hat{R}_b = 31500 \Omega_b h^2 \left(\frac{T_{\text{CMB}}}{2.7} \right)^{-4}. \quad (52)$$

The comoving distance and the comoving sound horizon are evaluated at the photon-decoupling redshift z_* , calculated in Appendix E of [53] with

$$z_* = 1048[1 + 0.00124(\Omega_b h^2)^{-0.738}][1 + g_1(\Omega_m h^2)^{g_2}],$$

where

$$g_1 = 0.0783(\Omega_b h^2)^{-0.238}[1 + 39.5(\Omega_b h^2)^{-0.763}]^{-1},$$

$$g_2 = 0.560[1 + 21.1(\Omega_b h^2)^{1.81}]^{-1}.$$

Let us recall that the shift parameters depend on the position of the CMB acoustic peaks, which are functions of the geometry of the model considered. For that reason, they can be used to discriminate between different models or different values of the free parameters \mathbf{x} , which includes Ω_b in this case. A complete and detailed description of these parameters and those that follow can be found in [52,54].

D. Baryon acoustic oscillations data

The last set of data addresses BAOs, which are fluctuations in the density of visible baryonic matter as a consequence of acoustic density waves in the primordial plasma. Accordingly, there is a distance associated with the maximum distance that acoustic waves can travel through this media until the plasma cooled at the recombination moment, where it became a soup of neutral atoms and the expansion of plasma density waves stopped and they got frozen. That being so, the mentioned distance can be used as a standard ruler.

We will use five sets of data, collected by different observational missions. Let us give now relevant details.

- (i) WiggleZ: These are data coming from the WiggleZ Dark Energy survey [55], which are evaluated at redshifts $z_w = (0.44, 0.66, 0.73)$ as shown in Table 1 of [56]. Following that work, we will consider two quantities: the acoustic parameter given by

$$A(z, \mathbf{x}) = 100 \sqrt{\Omega_m h^2} \frac{D_V(z, \mathbf{x})}{cz} \quad (53)$$

and the Alcock-Paczynski distortion parameter

$$F(z, \mathbf{x}) = (1+z) \frac{D_A(z, \mathbf{x})H(z, \mathbf{x})}{c}, \quad (54)$$

where D_A is the angular diameter distance,

$$D_A(z) = \frac{1}{1+z} \int_0^z \frac{cdz'}{H_0 E(z', \mathbf{x})}, \quad (55)$$

and D_V is the geometric mean of the longitudinal (D_A) and radial ($c/H(z)$) BAO modes, defined as

$$D_V(z, \mathbf{x}) = \left[(1+z)^2 D_A^2(z, \mathbf{x}) \frac{cz}{H(z, \mathbf{x})} \right]^{1/3}. \quad (56)$$

Consequently, we have two observational parameters, that is, $A(z_w)$ and $F(z_w)$ which can be compared with the theoretical value drawn from the model under study with a specific \mathbf{x} , and allowing us to construct a new $\Delta\mathcal{F}_w$. In these cases, we define χ_w^2 as

$$\chi_w^2 = (\Delta\mathcal{F}_w)^T \cdot C_w^{-1} \cdot \Delta\mathcal{F}_w, \quad (57)$$

where C_w^{-1} is a matrix given in Table 2 of [56].

- (ii) BOSS: In this case, we consider the data from the SDSS-III Baryon Oscillation Spectroscopy Survey (BOSS) DR12 described in [57]. We proceed analogously to the WiggleZ case but now we have $z_B = (0.38, 0.51, 0.61)$, whereas the fundamental parameters are

$$D_M(z, \mathbf{x}) \frac{r_s^{\text{fid}}(z_d)}{r_s(z_d, \mathbf{x})}, \quad H(z, \mathbf{x}) \frac{r_s(z_d, \mathbf{x})}{r_s^{\text{fid}}(z_d)}, \quad (58)$$

where $D_M(z) = r(z)$ is the comoving distance, $r_s(z_d, \mathbf{x})$ denotes the sound horizon defined as Eq. (50) but evaluated at the dragging redshift z_d , and $r_s^{\text{fid}}(z_d)$ is the same parameter but calculated for a given fiducial cosmological model which in this specific case is equal to 147.78 Mpc. Clearly, the first step involves calculating the redshift of the drag epoch z_d , which can be done considering the approximation [58]

$$z_d = \frac{1925(\Omega_m h^2)^{0.251}}{1 + 0.659(\Omega_m h^2)^{0.828}} [1 + b_1(\Omega_b h^2)^{b_2}], \quad (59)$$

where b_1 and b_2 are factors calculated as follows:

$$b_1 = 0.313(\Omega_m h^2)^{-0.419} \times [1 + 0.607(\Omega_m h^2)^{0.6748}], \quad (60)$$

$$b_2 = 0.238(\Omega_m h^2)^{0.223}. \quad (61)$$

Once more, we will define

$$\chi_B^2 = (\Delta\mathcal{F}_B)^T \cdot C_B^{-1} \cdot \Delta\mathcal{F}_B, \quad (62)$$

where $\Delta\mathcal{F}_B$ is the difference between the observational data and the resulting value for \mathbf{x} , and C_B^{-1} is the inverse of the covariance matrix given in Table 8 of [57].

- (iii) eBOSS: The extended Baryon Oscillation Spectroscopy Survey (eBOSS) gives us one more data point [59],

$$D_V(z = 1.52) = 3843 \pm 147 \frac{r_s(z_d)}{r_s^{\text{fid}}(z_d)} \text{Mpc}. \quad (63)$$

Our function χ_{eB}^2 gets a simpler expression that in other cases, as the matrix notation is not necessary, and we simply have

$$\chi_{eB}^2 = \frac{\Delta\mathcal{F}_{eB}^2}{\sigma_{eB}^2}, \quad (64)$$

where σ_{eB}^2 is the error in the datum.

- (iv) BOSS-Lyman α : Another set of data is Quasar-Lyman α Forest from SDSS-III BOSS DR11 [60] which contributes two new data points to the analysis,

$$\frac{D_M(z = 2.34, \mathbf{x})}{r_s(z_d, \mathbf{x})} = 36.98_{-1.18}^{+1.26}, \quad (65)$$

$$\frac{c}{H(z = 2.34, \mathbf{x}) r_s(z_d, \mathbf{x})} = 9.00_{-0.22}^{+0.22}, \quad (66)$$

and its χ^2 is defined as usual.

- (v) Finally, we consider the voids-galaxy cross-correlation data from [61]. This set gives us two new data points at $z = 0.57$ which are

$$\frac{D_A(z = 0.57, \mathbf{x})}{r_s(z_d, \mathbf{x})} = 9.383 \pm 0.077, \quad (67)$$

$$H(z = 0.57, \mathbf{x}) r_s(z_d, \mathbf{x}) = (14.05 \pm 0.14) \frac{10^3 \text{ km}}{\text{s}}, \quad (68)$$

and the same usual definition applies to its χ^2 .

VI. RESULTS

After having set forth our statistical procedure along with a detailed outline of the astrophysical probes chosen, we can now present the results of our research.

We stress once more that a key aspect is the comparison of the novel $f(Q)$ scenario under consideration with the Λ CDM standard. To this end, we simply perform all the tests on this scenario as well.

From a very wide perspective, we could also wonder about the peculiar case of our $f(Q)$ model that follows from setting $\Omega_\Lambda = 0$. In principle, this scenario would be of interest as to avoid the problems associated with the cosmological constant. Although some insight into this particular setting can be easily drawn from the more general

TABLE I. MCMC best fits and errors. Quantities in italic correspond to secondary parameters.

		Pantheon	Hubble	CMB	BAO	Total
Ω_m	Λ CDM	$0.298^{+0.022}_{-0.021}$	$0.327^{+0.066}_{-0.056}$	$0.316^{+0.007}_{-0.007}$	$0.320^{+0.016}_{-0.015}$	$0.323^{+0.005}_{-0.005}$
	$f(Q)_{\Omega_\Lambda \neq 0}$	$0.337^{+0.075}_{-0.073}$	$0.341^{+0.070}_{-0.060}$	$0.346^{+0.092}_{-0.080}$	$0.323^{+0.020}_{-0.017}$	$0.325^{+0.007}_{-0.007}$
	$f(Q)_{\Omega_\Lambda = 0}$	$0.400^{+0.024}_{-0.024}$	$0.350^{+0.057}_{-0.049}$	$0.238^{+0.006}_{-0.006}$	$0.348^{+0.016}_{-0.016}$	$0.285^{+0.004}_{-0.004}$
Ω_b	Λ CDM	$0.0491^{+0.0006}_{-0.0006}$	$0.063^{+0.012}_{-0.031}$	$0.0496^{+0.0004}_{-0.0004}$
	$f(Q)_{\Omega_\Lambda \neq 0}$	$0.057^{+0.014}_{-0.012}$	$0.081^{+0.019}_{-0.036}$	$0.0501^{+0.0010}_{-0.0010}$
	$f(Q)_{\Omega_\Lambda = 0}$	$0.0371^{+0.0005}_{-0.0005}$	$0.042^{+0.011}_{-0.021}$	$0.0407^{+0.0004}_{-0.0004}$
h	Λ CDM	...	$0.678^{+0.031}_{-0.031}$	$0.675^{+0.005}_{-0.005}$	>0.65	$0.670^{+0.003}_{-0.003}$
	$f(Q)_{\Omega_\Lambda \neq 0}$...	$0.674^{+0.039}_{-0.054}$	$0.645^{+0.090}_{-0.071}$	>0.62	$0.667^{+0.007}_{-0.007}$
	$f(Q)_{\Omega_\Lambda = 0}$...	$0.703^{+0.029}_{-0.030}$	$0.777^{+0.007}_{-0.007}$	>0.70	$0.730^{+0.004}_{-0.004}$
Ω_Λ	Λ CDM	$0.701^{+0.021}_{-0.022}$	$0.673^{+0.056}_{-0.066}$	$0.684^{+0.007}_{-0.007}$	$0.680^{+0.015}_{-0.016}$	$0.677^{+0.005}_{-0.005}$
	$f(Q)_{\Omega_\Lambda \neq 0}$	$0.43^{+0.47}_{-0.49}$	$0.64^{+0.59}_{-0.60}$	$0.87^{+0.43}_{-0.57}$	$1.11^{+0.21}_{-0.18}$	$0.701^{+0.054}_{-0.053}$
	$f(Q)_{\Omega_\Lambda = 0}$
Ω_Q	Λ CDM
	$f(Q)_{\Omega_\Lambda \neq 0}$	$0.23^{+0.42}_{-0.40}$	$0.03^{+0.58}_{-0.61}$	$-0.22^{+0.65}_{-0.52}$	$-0.43^{+0.18}_{-0.22}$	$-0.027^{+0.057}_{-0.058}$
	$f(Q)_{\Omega_\Lambda = 0}$	$0.599^{+0.023}_{-0.024}$	$0.650^{+0.049}_{-0.057}$	$0.762^{+0.006}_{-0.006}$	$0.651^{+0.016}_{-0.016}$	$0.715^{+0.004}_{-0.004}$
χ^2	Λ CDM	1035.77	14.49	0.001	16.55	1072.19
	$f(Q)_{\Omega_\Lambda \neq 0}$	1035.72	14.40	0.005	11.34	1072.01
	$f(Q)_{\Omega_\Lambda = 0}$	1036.48	14.53	0.003	51.34	1207.96
$\mathcal{B}_{\Lambda\text{CDM}}^i$	Λ CDM	1
	$f(Q)_{\Omega_\Lambda \neq 0}$	0.76
	$f(Q)_{\Omega_\Lambda = 0}$	3×10^{-30}
$\ln \mathcal{B}_{\Lambda\text{CDM}}^i$	Λ CDM	0
	$f(Q)_{\Omega_\Lambda \neq 0}$	-0.27
	$f(Q)_{\Omega_\Lambda = 0}$	-68

$f(Q)$ one, we treat it in full so that our conclusions are more complete and precise.

The best fits of (the three) models we analyze are shown in Table I. Let us emphasize that Ω_Q is a characteristic parameter of the $f(Q)$ scenario, a signature of it that does not appear at all in the Λ CDM setting.

For additional discernment, we present the marginalized confidence contours directly as drawn from the MCMC procedure providing our best fits. This supplies visual hints of the complementarity of different data sets, their constraining power, and correlation among parameters. The comparison of the contour plots for Λ CDM and $f(Q)$ with $\Omega_\Lambda \neq 0$ can be found in Fig. 1, while specific results of the $f(Q)$ model are presented separately in Fig. 2. Finally, results for $f(Q)$ with $\Omega_\Lambda = 0$ are shown in Fig. 3. For each individual data set or data set combination, we draw the contours by choosing two shades of a single color, and we let the dark and light hues represent the 1σ and 2σ regions, respectively.

One of the main conclusions of the MCMC analysis is that in the case of $f(Q)$ with $\Omega_\Lambda \neq 0$ the combination of data sets yields a tiny negative value of Ω_Q . Specifically, it lies in a significantly wide uncertainty range that makes it

compatible with a null value at the 1σ level (see Table I and the black contour in Fig. 2). This compatibility with a vanishing Ω_Q applies for all the separate data sets except for BAO, which not only bet on a larger negative value only compatible with $\Omega_Q = 0$ at the 2σ level, but also exhibit much lower errors (at least twice smaller) than other probes. The large uncertainty in Ω_Q can undoubtedly be associated to that in Ω_Λ . It is visually manifest that the two parameters are mutually quite (anti)correlated for all data sets, as the inclination of the contours is very close to -45° . This significant negative correlation, expected from Eq. (29), makes the large degree of uncertainty in the Ω_Λ induce the same behavior on Ω_Q . Interestingly, the negative best fit value of Ω_Q hints at the interest of exploring and characterizing sudden future singularities in these models.

A second outcome is that, independently of the values of Ω_Λ and Ω_Q , the fits of the other two parameters, Ω_m and h , are very similar in the $f(Q)$ and Λ CDM scenarios. This makes sense considering previous arguments, because shifts in Ω_Λ are reabsorbed into Ω_Q and vice versa, affecting quite little the rest of parameters. A reflection of this fact are the very similar χ^2 values displayed by both models in Table I.

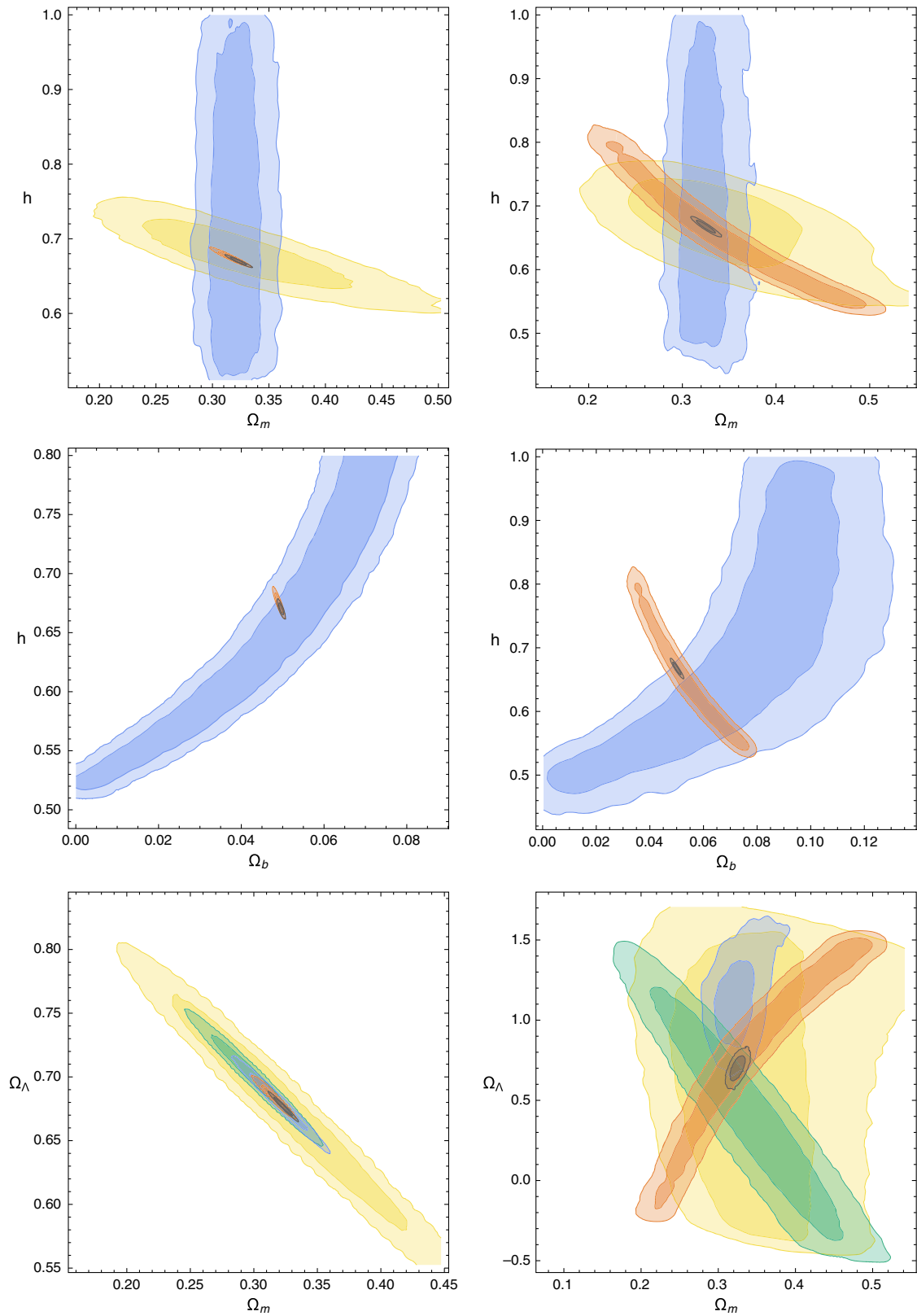


FIG. 1. Contour plots for the Λ CDM model (left column) and the $f(Q)$ model with $\Omega_\Lambda \neq 0$ (right column) with the following color scheme: green, SNeIa; yellow, Hubble data; orange, Planck 2018 CMB; blue, BAO data; black, all sets of data. As SNeIa are (of course) unable to fix the value h , their contours are missing from those plots where constraints on h are shown; for the same rationality, both SNeIa and Hubble contours are absent from plots showing constraints on Ω_b .

But we may also note that, although the Λ CDM and $f(Q)$ with $\Omega_\Lambda \neq 0$ models yield similar best fits of Ω_m and Ω_Λ , the distinctive feature encoded in Ω_Q changes quite significantly the correlations between those two parameters (see the bottom row of Fig. 1).

However, the behavior of Ω_m and h is approximately similar in both models (see the top row of Fig. 1) in a broad sense and in particular in what concerns the correlation among the two parameters. Still there is a noticeable difference, which is the quite larger uncertainty on Ω_m as associated with CMB data in the case of $f(Q)$ with $\Omega_\Lambda \neq 0$. We infer accordingly that the roles of Ω_m and h seem to be quite similar at low redshifts, but the same does not apply at high redshifts for what Ω_m is concerned.

Recalling the Bayes factors, the conclusion is (again) that, within the current data sets, we are not able to distinguish one model from the other. This reasoning is obviously drawn from a background examination, a perturbative one might propound more refined pieces of information (some results along this route were sketched in [21]).

We now may come back the possibility of imposing $\Omega_\Lambda = 0$. Figure 2 provides insight on this matter, as it shows that Ω_Λ is enormously correlated with Ω_Q ; for that reason, that parameter could in principle take the role of the cosmological constant and thus give the same evolution, but then the model would then be irreducible to Λ CDM, as it can be seen by looking at Eq. (31). However, a look at the locus on the contours of Fig. 2 which corresponds to $\Omega_\Lambda = 0$ suggest that this value is clearly disfavored. Nevertheless, we have decided to perform a direct MCMC analysis to confirm such concerns (see Table II).

The strong tension among all single data sets in this restricted scenario becomes manifest in Fig. 3. Paradoxically, the CMB constraints are much better than those derived in the $f(Q)$ case with $\Omega_\Lambda \neq 0$, but they require an abnormally low

value for Ω_m which is not consistent with any of the other probes considered. Moreover, although the single χ^2 is comparable with those from other frameworks, we must note that BAOs are produce very poor constraints, and that the best fit χ^2 coming from the joint use of all the probes is much larger. If we finally look at the values of the Bayes factors, we can see how this scenario is frankly statistically disfavored with respect to the other cases.

In addition to these results, we can compute the cosmographic parameters deceleration q_0 , jerk j_0 , and snap s_0 to add more elements to the comparison between the kinematics of the two models. Table II summarizes our findings: best fits all share an uncertainty which is much larger in the $f(Q)$ case than in the Λ CDM case, and with the latter estimations which fall completely within their respective counterparts in the former ones.

Finally, and to close this section, we confront once again our modified gravity scenario with Λ CDM by rewriting it as a model fueled by dark matter, radiation and dark energy following, for instance [62–65], by setting

$$p_{\text{eff}} = w_{\text{eff}}\rho_{\text{eff}} \quad (69)$$

and

$$H^2 = H_0^2[\Omega_m(1+z)^3 + \Omega_r(1+z)^4] + \frac{8\pi G}{3}\rho_{\text{eff}}. \quad (70)$$

If we combine the last two expressions with the continuity equation, Eq. (25), we finally write

$$w_{\text{eff}}(z) = \frac{2(1+z)\frac{d\ln E(z)}{dz} - E^{-2}(z)\Omega_r(1+z)^4 - 3}{3(1 - E^{-2}(z)[\Omega_m(1+z)^3 + \Omega_r(1+z)^4])}. \quad (71)$$

The explicit expression of w_{eff} for our modified gravity model is too complicated for it to convey readily usable

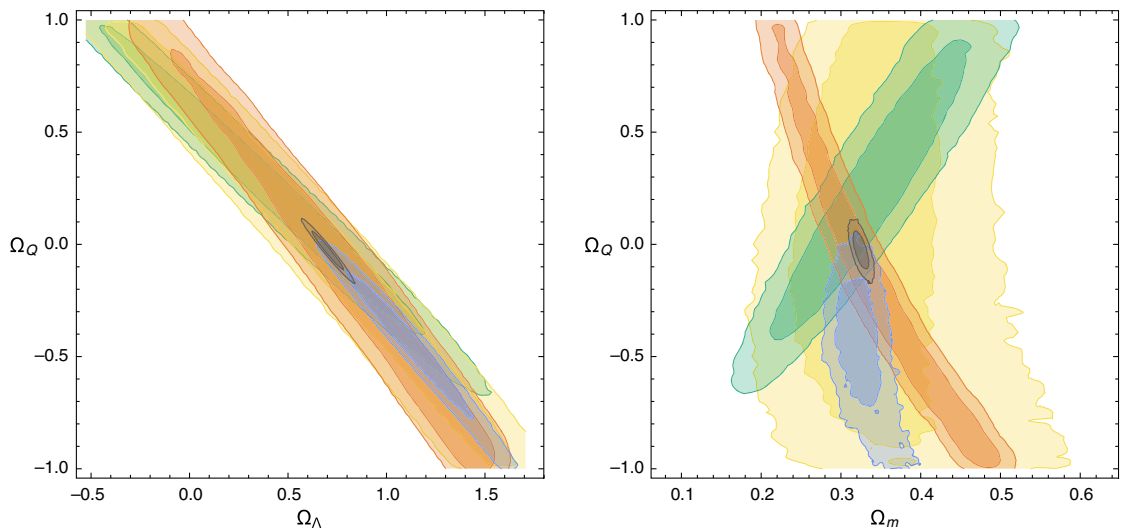


FIG. 2. Contour plots for the $f(Q)$ model with $\Omega_\Lambda \neq 0$ with the following color scheme: green, SNIa; yellow, Hubble data; orange, Planck 2018 CMB; blue, BAO data; black, all sets of data.

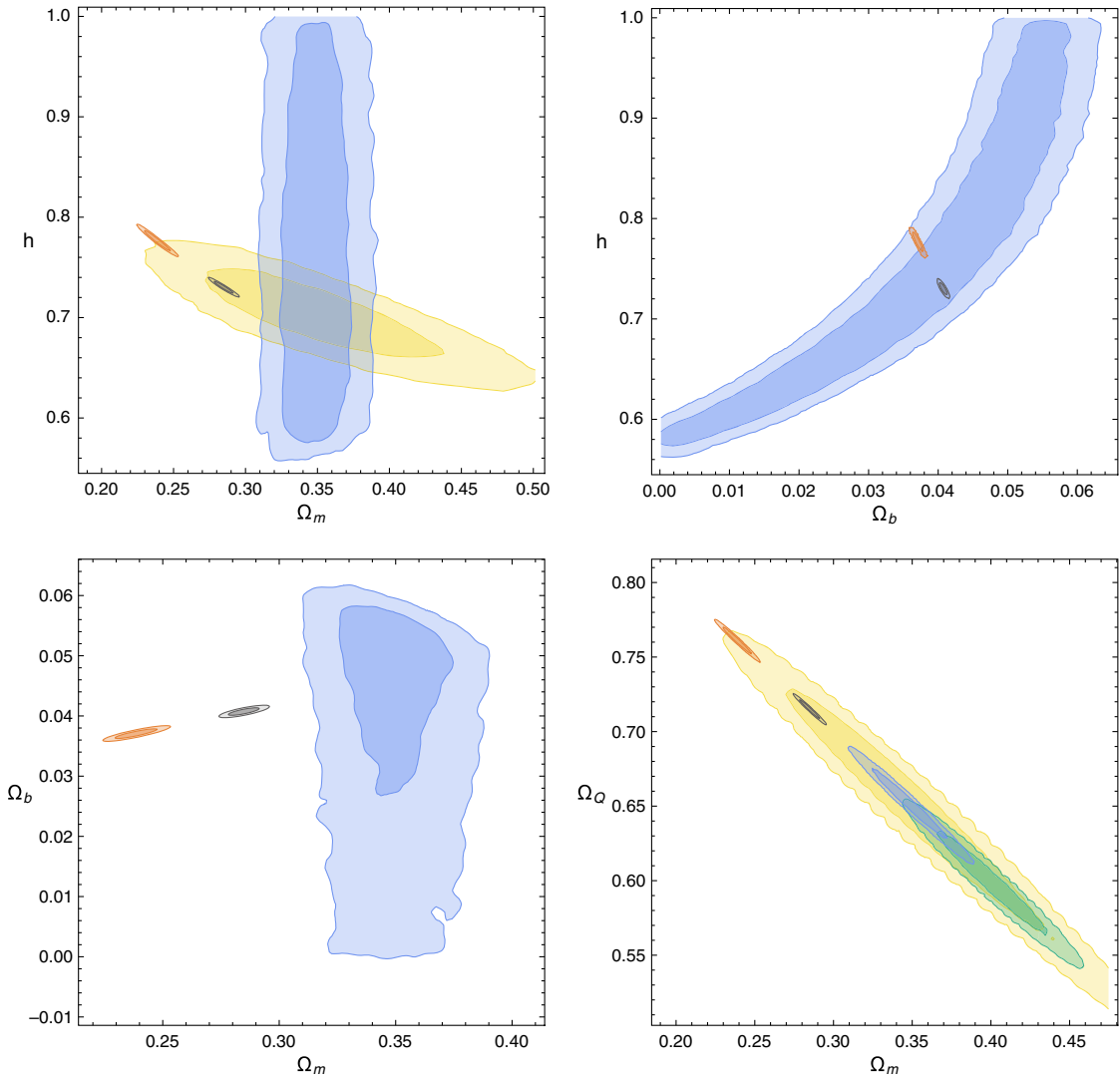


FIG. 3. Contour plots for the $f(Q)$ model with $\Omega_\Lambda = 0$ using the following color scheme: green, SNIa; yellow, Hubble data; orange, Planck 2018 CMB; blue, BAO data; black, all sets of data.

information, so we regard it sufficient to plot it as a function of a in Fig. 4 using the best fit values coming from the MCMC. In addition, and once more with the results of the MCMC analysis, we are able to calculate the value of w_{eff} at the present day for the $f(Q)$ model,

$$w_{\text{eff}}|_{z=0} = -0.987^{+0.032}_{-0.027}. \quad (72)$$

Once again, we find an indication that the best fit values of the parameters of our model are very similar to those of

TABLE II. Best fits of the cosmographic parameters.

	q_0	j_0	s_0
ΛCDM	$-0.515^{+0.007}_{-0.007}$	$1.000186^{+2 \times 10^{-6}}_{-2 \times 10^{-6}}$	$-0.454^{+0.021}_{-0.021}$
$f(Q)_{\Omega_\Lambda \neq 0}$	$-0.499^{+0.040}_{-0.035}$	$0.973^{+0.053}_{-0.081}$	$-0.453^{+0.029}_{-0.039}$

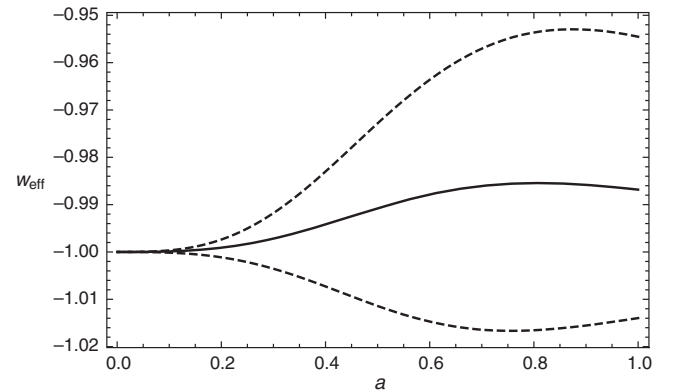


FIG. 4. Evolution of w_{eff} as function of a . The solid line is the value as drawn from the best fit, while the dashed lines mark the boundaries of the confidence interval.

Λ CDM; in fact, $w_{\text{eff}} = -1$ is perfectly inside the 1σ interval.

VII. SUMMARY AND CONCLUSIONS

Recent works in the field have been inspired by the realization that, in the symmetric teleparallel framework, the GR Lagrangian density can be written by basically replacing the scalar of curvature built from the Levi-Civita connection with the nonmetricity Q (up to small details which are not really relevant for a summary level of discussion).

The former framework can be generalized upon replacement of Q with a specific $f(Q)$ given by Eq. (21) which reproduces the Λ CDM background behavior. Interestingly, the fact that this new setup is not exactly a GR one might have implications at the perturbative level, which is (also) beyond our specific concerns. The particular action considered at this intermediate test allows us to make progress toward yet another form of $f(Q)$, which becomes the core of the present work; we present it in Eq. (22) and it lets draw an exact expression for the Hubble parameter under some parameter specifications. The grand picture of this choice is that it resembles standard evolutions and is therefore worth testing observationally. To that end, we resort to the MCMC method as to constraint the free parameters in the theory and compare the values obtained with those of the Λ CDM scenario.

Our main conclusion is that the parameter which encodes the difference between the two evolutions at the background level is very close to zero when all data sets are combined. This parameter, which we have dubbed Ω_Q , gets positive best fit values for some data sets while it is negative for others, but in all cases the errors make the best fit perfectly compatible with a null value; thus, an overall

smaller best fit (almost zero value) is a most admissible consequence. The same conclusion follows from the Bayesian evidence: according to Jeffreys' scale, no model is preferred over the other.

A complementary study of the cosmographic parameters yields values which again only reflect the striking similarity of the best fits between Λ CDM and our $f(Q)$. Note in this respect that, for the modified gravity model, these parameters are more poorly constrained as their complexity penalizes error propagation. Finally, and for the sake of further interpretation of the kind of evolution our best fit scenario depicts, we have computed the corresponding w_{eff} . As expected, the value is very close to -1 .

For all these reasons, we have seen that a yet another (promising/intriguing) cosmological candidate to become an alternative to Λ CDM cannot be considered a real challenger, at least at the background level.

ACKNOWLEDGMENTS

We are grateful to José Beltrán Jiménez and Marco de Cesare for enlightening discussions. I. A. and R. L. thank Fernando Díez Varela for motivating conversations. This paper is based upon work from CANTATA COST (European Cooperation in Science and Technology) action CA15117, EU Framework Programme Horizon 2020. I. A. was funded by Fundação para a Ciência e a Tecnologia Grant No. PD/BD/114435/2016 under the IDPASC PhD Program. The work of R. L. was supported by the Spanish Ministry of Science and Innovation through research projects FIS2017-85076-P (comprising FEDER funds) and also by the Basque Government and Generalitat Valenciana through research projects GIC17/116-IT956-16 and PROMETEO/2020/079, respectively.

-
- [1] A. Einstein, *Sitzungsber. Preuss. Akad. Wiss. Berlin (Math. Phys.)* **1915**, 844 (1915).
 - [2] A. Einstein, *Sitzungsber. Preuss. Akad. Wiss. Berlin (Math. Phys.)* **1915**, 778 (1915); **1915**, 799(A) (1915).
 - [3] C. M. Will, *Living Rev. Relativity* **17**, 4 (2014).
 - [4] E. Berti *et al.*, *Classical Quantum Gravity* **32**, 243001 (2015).
 - [5] S. M. Carroll, *Living Rev. Relativity* **4**, 1 (2001).
 - [6] P. J. E. Peebles and B. Ratra, *Rev. Mod. Phys.* **75**, 559 (2003).
 - [7] S. Weinberg, *Rev. Mod. Phys.* **61**, 1 (1989).
 - [8] T. Padmanabhan, *Phys. Rep.* **380**, 235 (2003).
 - [9] S. M. Carroll, eConf **C0307282**, TTH09 (2003); *AIP Conf. Proc.* **743**, 16 (2004).
 - [10] E. Bianchi and C. Rovelli, [arXiv:1002.3966](https://arxiv.org/abs/1002.3966).
 - [11] P. Bull *et al.*, *Phys. Dark Universe* **12**, 56 (2016).
 - [12] S. Capozziello, *Int. J. Mod. Phys. D* **11**, 483 (2002).
 - [13] T. Clifton, P. G. Ferreira, A. Padilla, and C. Skordis, *Phys. Rep.* **513**, 1 (2012).
 - [14] A. Joyce, B. Jain, J. Khoury, and M. Trodden, *Phys. Rep.* **568**, 1 (2015).
 - [15] T. Harko and F. S. N. Lobo, *Extensions of $f(R)$ Gravity* (Cambridge University Press, Cambridge, United Kingdom, 2018).
 - [16] S. Capozziello and M. Francaviglia, *Gen. Relativ. Gravit.* **40**, 357 (2008).
 - [17] T. P. Sotiriou and S. Liberati, *Ann. Phys. (Amsterdam)* **322**, 935 (2007).
 - [18] J. B. Jiménez, L. Heisenberg, and T. S. Koivisto, *Universe* **5**, 173 (2019).
 - [19] J. Beltrán Jiménez, L. Heisenberg, D. Iosifidis, A. Jiménez-Cano, and T. S. Koivisto, *Phys. Lett. B* **805**, 135422 (2020).

- [20] I. Mol, *Adv. Appl. Cliord Algebras* **27**, 2607 (2017).
- [21] J. Beltrán Jiménez, L. Heisenberg, T. S. Koivisto, and S. Pekar, *Phys. Rev. D* **101**, 103507 (2020).
- [22] F. W. Hehl, J. McCrea, E. W. Mielke, and Y. Ne'eman, *Phys. Rep.* **258**, 1 (1995).
- [23] L. Järv, M. Rünkla, M. Saal, and O. Vilson, *Phys. Rev. D* **97**, 124025 (2018).
- [24] G. J. Olmo, *Int. J. Mod. Phys. D* **20**, 413 (2011).
- [25] G. J. Olmo, *Phys. Rev. D* **72**, 083505 (2005).
- [26] R. Weitzenböck, *Invariantentheorie* (Noordhoff, Gronningen, 1923).
- [27] R. Aldrovandi and J. G. Pereira, *Teleparallel Gravity: An Introduction* (Springer, New York, 2013), Vol. 173.
- [28] J. Maluf, *J. Math. Phys. (N.Y.)* **35**, 335 (1994).
- [29] J. W. Maluf, *J. Math. Phys. (N.Y.)* **36**, 4242 (1995).
- [30] V. de Andrade and J. Pereira, *Phys. Rev. D* **56**, 4689 (1997).
- [31] U. Muench, F. Gronwald, and F. W. Hehl, *Gen. Relativ. Gravit.* **30**, 933 (1998).
- [32] K. Hayashi and T. Shirafuji, *Phys. Rev. D* **19**, 3524 (1979); **24**, 3312(A) (1982).
- [33] E. W. Mielke, *Ann. Phys. (N.Y.)* **219**, 78 (1992).
- [34] J. M. Nester and H.-J. Yo, *Chin. J. Phys. (Taipei)* **37**, 113 (1999).
- [35] R. Lazkoz, F. S. N. Lobo, M. Ortiz-Baños, and V. Salzano, *Phys. Rev. D* **100**, 104027 (2019).
- [36] J. Beltrán Jiménez, L. Heisenberg, and T. S. Koivisto, *J. Cosmol. Astropart. Phys.* **08** (2018) 039.
- [37] L. Fernandez-Jambrina and R. Lazkoz, *Phys. Lett. B* **670**, 254 (2009).
- [38] R. Lazkoz, V. Salzano, and I. Sendra, *Phys. Lett. B* **694**, 198 (2011).
- [39] S. Capozziello, R. Lazkoz, and V. Salzano, *Phys. Rev. D* **84**, 124061 (2011).
- [40] S. Nesseris and J. Garcia-Bellido, *J. Cosmol. Astropart. Phys.* **08** (2013) 036.
- [41] H. Jeffreys, *Theory of Probability*, 3rd ed. (Oxford University Press, Oxford, United Kingdom, 1961).
- [42] M. Visser, *Gen. Relativ. Gravit.* **37**, 1541 (2005).
- [43] C. Cattoen and M. Visser, *Classical Quantum Gravity* **24**, 5985 (2007).
- [44] D. M. Scolnic *et al.*, *Astrophys. J.* **859**, 101 (2018).
- [45] A. Conley *et al.* (SNLS Collaboration), *Astrophys. J. Suppl. Ser.* **192**, 1 (2011).
- [46] R. Jimenez and A. Loeb, *Astrophys. J.* **573**, 37 (2002).
- [47] M. Moresco, R. Jimenez, A. Cimatti, and L. Pozzetti, *J. Cosmol. Astropart. Phys.* **03** (2011) 045.
- [48] M. Moresco *et al.*, *J. Cosmol. Astropart. Phys.* **08** (2012) 006.
- [49] M. Moresco, L. Pozzetti, A. Cimatti, R. Jimenez, C. Maraston, L. Verde, D. Thomas, A. Citro, R. Tojeiro, and D. Wilkinson, *J. Cosmol. Astropart. Phys.* **05** (2016) 014.
- [50] M. Moresco, *Mon. Not. R. Astron. Soc.* **450**, L16 (2015).
- [51] Y. Wang and M. Dai, *Phys. Rev. D* **94**, 083521 (2016).
- [52] Z. Zhai and Y. Wang, *J. Cosmol. Astropart. Phys.* **07** (2019) 005.
- [53] W. Hu and N. Sugiyama, *Astrophys. J.* **471**, 542 (1996).
- [54] E. Komatsu *et al.* (WMAP Collaboration), *Astrophys. J. Suppl. Ser.* **180**, 330 (2009).
- [55] C. Blake *et al.*, *Mon. Not. R. Astron. Soc.* **418**, 1707 (2011).
- [56] C. Blake *et al.*, *Mon. Not. R. Astron. Soc.* **425**, 405 (2012).
- [57] S. Alam *et al.* (BOSS Collaboration), *Mon. Not. R. Astron. Soc.* **470**, 2617 (2017).
- [58] D. J. Eisenstein and W. Hu, *Astrophys. J.* **496**, 605 (1998).
- [59] M. Ata *et al.*, *Mon. Not. R. Astron. Soc.* **473**, 4773 (2018).
- [60] V. de Sainte Agathe *et al.*, *Astron. Astrophys.* **629**, A85 (2019).
- [61] S. Nadathur, P. M. Carter, W. J. Percival, H. A. Winther, and J. Bautista, *Phys. Rev. D* **100**, 023504 (2019).
- [62] A. A. Starobinsky, *JETP Lett.* **68**, 757 (1998).
- [63] T. Nakamura and T. Chiba, *Mon. Not. R. Astron. Soc.* **306**, 696 (1999).
- [64] D. Huterer and M. S. Turner, *Phys. Rev. D* **60**, 081301 (1999).
- [65] R. Lazkoz and E. Majerotto, *J. Cosmol. Astropart. Phys.* **07** (2007) 015.